

Dependence of the contact angle on the molecular structure of poly(propene-*alt*-*N*-maleimide) and poly(styrene-*alt*-*N*-maleimide) copolymers

T. GIETZELT

Karlsruhe Research Center, Institute of Materials Research III, PO Box 3640,
76021 Karlsruhe, Germany
E-mail: thomas.gietzelt@imf.fzk.de

Dynamic contact angle measurements on poly(propene-*alt*-*N*-maleimide) and poly(styrene-*alt*-*N*-maleimide) copolymers are presented. The copolymers were altered by side chains of saturated hydrocarbons of increasing length. Films of these copolymers were formed on silica wafers by casting from polymer solutions. Axisymmetric Drop Shape Analysis for Profiles (ADSA-P) was used for low rate dynamic contact angle measurements. The solid surface tension γ_{SV} was calculated using an "Equation of State". For poly(propene-*alt*-*N*-maleimide) copolymers increasing length of the side chains lead to an increasing contact angle. The solid surface tension γ_{SV} varied in the range from 22.6 to 41.5 mJ/m². For a side chain with 12 carbon atoms the surface tension γ_{SV} is at the value reported in the literature for surfaces consisting mainly of CH₃-groups. The wetting behavior for poly(styrene-*alt*-*N*-maleimide) copolymers, however, showed a very strange behavior for water and glycerol, respectively. No trend of the contact angle versus the length of the side chain could be found. Instead, two different ranges of the contact angle appeared. At three carbon atoms it is inconsistent. Molecular modeling suggested a conformation for poly(styrene-*alt*-*N*-maleimides) to explain the unexpected behavior. This model was supported by wide angle X-ray diffraction (WAXS). A similar conformation was also suggested by Natta. From this it can be concluded that contact angle measurements are very sensitive to structural changes and represent a simple, yet powerful technique to characterize solid surfaces. © 2001 Kluwer Academic Publishers

1. Introduction

In [1] many experiments of low rate dynamic contact angle measurements on poly(styrene-*alt*-*N*-((*n*-hexyl)/(10carboxydecyl)90/10)-maleimide) were done by Kwok to show that the "Equation of State" derived by Neumann [2] works well. According to Young-Equation (1) it was shown that there are too many parameters and γ_{SL} depends on γ_{SV} and γ_{LV} , respectively (2).

$$\text{Young Equation } \gamma_{LV} \cos \theta = \gamma_{SV} - \gamma_{SL} \quad (1)$$

$$\text{Dependence of } \gamma_{SL} \quad \gamma_{SL} = f(\gamma_{SV}, \gamma_{LV}) \quad (2)$$

γ_{SL} —surface tension solid/liquid

γ_{SV} —surface tension solid/vapor

γ_{LV} —surface tension liquid/vapor

Hence, here it was assumed that the derived "Equation of State" (3) was right.

Equation of State

$$\cos \theta = -1 + 2 \sqrt{\frac{\gamma_{SV}}{\gamma_{LV}}} e^{-0.0001247(\gamma_{LV} - \gamma_{SV})^2} \quad (3)$$

However, firstly one has to watch very carefully whether interactions of the testing liquid and the surface of the substrate like stick/slip or dissolution of the substrate appear. In these cases, the Young-Equation (1) is not satisfied and the contact angle cannot be used for the calculation of the solid surface tension γ_{SV} . Secondly, it is not suitable for practical reasons to use too many different liquids and to watch for interactions on each substrate. Hence, in this paper the testing liquids were limited to water and glycerol. Using these liquids poly(propene-*alt*-*N*-maleimide) and poly(styrene-*alt*-*N*-maleimide) copolymers modified with side chains of saturated hydrocarbons of different length were investigated. For both liquids it was shown by Kwok [1] that no interaction with the substrates occurred.

It was expected that an increasing length of saturated hydrocarbon side chains would lead to increasing

contact angles since it covers the polar maleimide groups. Consequently, the solid surface tension γ_{SV} should decrease. Thus, the solid surface tension γ_{SV} could be controlled in a subtle way. However, there is supposed to be a lower limit that is reached when the solid surface tension γ_{SV} is controlled predominantly by the nature of the side chains. It will be shown that this is the case for a dodecyl side chain containing 12 carbon atoms. At this point the solid surface tension γ_{SV} tends to reach a constant value.

For poly(styrene-*alt-N*-maleimide) copolymers, the intention was to show that the contact angle depends only on the length of the side chains, notwithstanding the copolymer backbone. However, the styrene ring is a very bulky group. Consequently the mobility of the backbone is restricted. The styrene ring leads to steric hindering of the copolymer backbone and shields the polar maleimide groups. For this reason, it was expected to find some higher contact angles for short side chains, compared to the propene-maleimide backbone. Additionally, it was expected that the dependence of the contact angle on the length of the side chains would have a smaller impact than for poly(propene-*alt-N*-maleimides), since the styrene groups contribute to the shielding of the polar maleimide groups too. First, poly(styrene-*alt-N*-maleimide) copolymers with saturated side chains containing one, three and six carbon atoms were investigated. It became obvious that there was an inconsistency for a side chain of three carbon atoms. Therefore, poly(styrene-*alt-N*-maleimide) copolymers with two, four and even without any carbon atoms in the side chain were prepared and investigated.

Since it is well known that the roughness of a surface can influence the contact angle, the smoothness of the copolymer films was investigated using atomic force microscopy (AFM) on the microscopic scale. For the macroscopic scale a mechanical method was employed. It was shown by Neumann and Bussher that for very smooth surfaces the roughness is not critical as far as the contact angle is concerned [3, 4].

2. Materials and preparation

2.1. Synthesizing copolymers

The starting raw materials were poly(propene-maleic-anhydride) and poly(styrene-maleic-anhydride), respectively. The imidization was carried out by polymer analogous reaction with primary amines. To ensure complete imidization a surplus of 10% of amines was added. Triethylamine was used as a catalyst. The medium for the chemical reaction was concentrated acetic acid. The experiments were carried out at 118 °C for a period of five hours. Afterwards the product was precipitated in water and dried in a vacuum oven at 60 °C for seven hours. According to Wienhold, the imidization degree after this treatment is better than 99% [5].

The advantage of this kind of reaction is that both the propene and styrene, respectively, as well as the maleimide parts of the molecule, alternate in a very strictly way. By this, copolymers with extremely well defined properties were received.

TABLE I Sample overview for poly(propene-*alt-N*-maleimides) and poly(styrene-*alt-N*-maleimides)

total length of the side chain <i>m</i>	poly(propene- <i>alt-N</i> -
1	methyl-maleimide)
3	(<i>n</i> -propyl)-maleimide)
6	(<i>n</i> -hexyl)-maleimide)
12	(<i>n</i> -dodecyl)-maleimide)
	poly(styrene- <i>alt-N</i> -
0	-maleimide)
1	-methylmaleimide)
2	-ethylmaleimide)
3	-(<i>n</i> -propyl)-maleimide)
4	-(<i>n</i> -butyl)-maleimide)
6	-(<i>n</i> -hexyl)-maleimide)

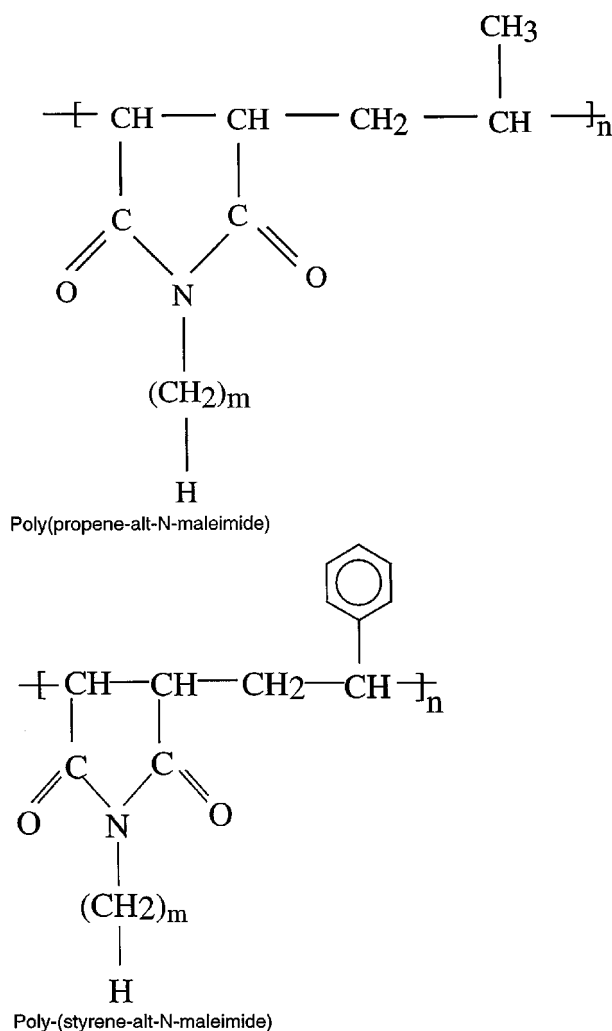


Figure 1 Chemical structures.

Fig. 1 shows the chemical structure of the copolymers in general. Table I gives a survey of all copolymers prepared and investigated.

2.2. Characterization of copolymers

Fig. 2 shows an ATR-FTIR plot of poly(propene-*alt-N*-(*n*-hexyl)-maleimide) and poly(styrene-*alt-N*-(*n*-hexyl)-maleimide), respectively. The large signal for the maleimide group is located at 1600 to 1740 cm^{-1} .

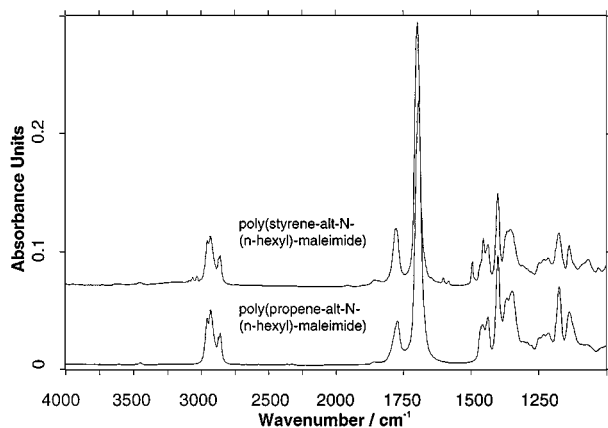


Figure 2 ATR-FTIR plot of poly(styrene-alt-*N*-(*n*-hexyl)-maleimide) (top) and poly(propene-alt-*N*-(*n*-hexyl)-maleimide) (bottom).

However, it can be seen that there are still anhydride peaks present between 1740 and 1850 cm^{-1} . This means that some residues of anhydride groups were left and not 100% of the anhydride was converted to maleimide. It is not possible to give an exact value of the anhydride, however, from investigations of Wienhold it was concluded that the imidization reaction is better than 99% [5]. For poly(styrene-alt-*N*-(*n*-hexyl)-maleimide) the anhydride peak is slightly higher than for poly(propene-alt-*N*-(*n*-hexyl)-maleimide). This indicates that the imidization was a little less than for the poly(propene-alt-*N*-maleimides). This effect may probably be attributed to the bulky structure of the styrene. Hence, the ability for moving and turning of backbone segments is reduced. Consequently, the accessibility of anhydride sites is restricted. Similar observations were made by Rätzsch *et al.* [6]. In this article the kinetic parameters for the reaction of anhydride copolymers to maleimide copolymers were determined as a function of different backbone sequences. It was shown that the velocity of the reaction decreases for the bulky poly(styrene-alt-*N*-anhydride) backbone due to steric

hindering. Primary amines cannot come into contact with the anhydride sites as good as for a poly(propene-alt-*N*-anhydride) backbone.

2.3. Sample preparation and characterization of copolymer films

The sample preparation was done by film casting as described in detail by Kwok [1]. Here a 4 wt-% tetrahydrofuran solution of the polymers was used. Some drops of the polymer solution were put onto a cleaned silicon wafer. The wafer was covered by a glass dish, in order to prevent fast evaporation of the solvent and precipitating dust on the film. By slow evaporation of the solvent, very smooth and homogeneous films were formed. There were colored fringes on the surface that are attributed to light refraction by tiny deviations of the thickness on the nanometer scale. By means of a touch step device DEKTAK 3030ST by VEECO using a diamond spike with a tip diameter of $2\text{ }\mu\text{m}$ and a load of 25 mg, the surface profile was evaluated. Fig. 3 shows a plot of a roughness measurement on this polymer film over a range of several millimeters. It can be seen that the roughness is at the most 50 nm, except for some peaks originating from dust particles. Fig. 4 shows a

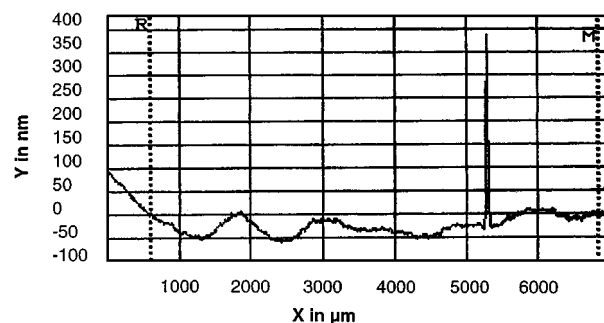


Figure 3 Plot of a touch-step device onto the surface of a cast film.

Roughness Analysis

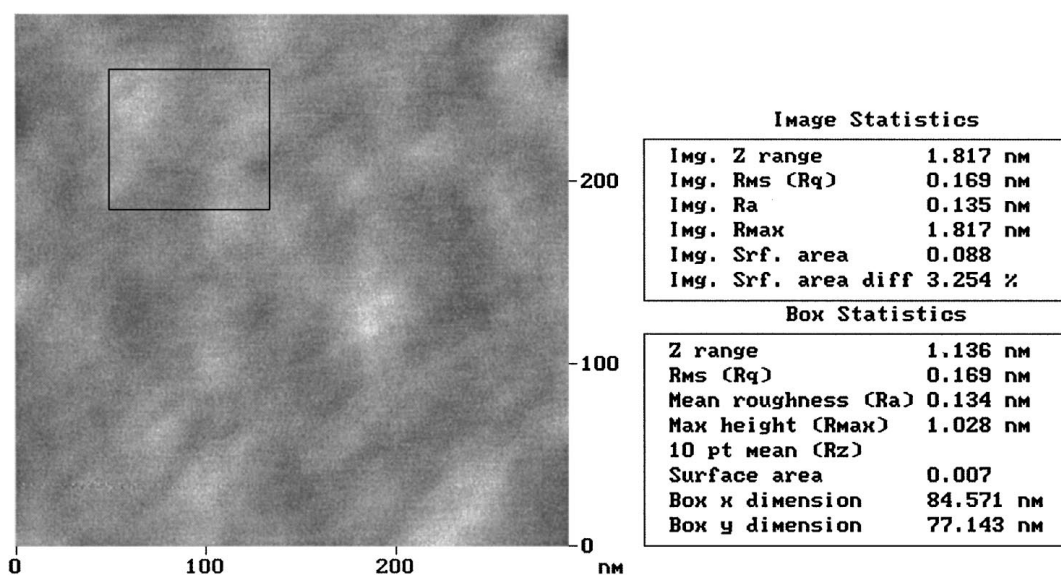


Figure 4 Plot of the film surface by an Atomic Force Microscope (200 nm).

roughness measurement by Atomic Force Microscopy. The roughness does not exceed 5 nm. First this seems to contradict the results obtained by the touch step device where the roughness is about ten times as high. However, one has to keep in mind that the lateral resolution of both methods is quite different. Therefore, the roughness values determined by both techniques are not comparable. The touch step device reflects a kind of uneven surface, possessing a long period of several hundred microns that is responsible for the concentric colored fringes on the substrate, which can be seen by the naked eye. This is probably due to material enrichment processes during solvent evaporation. Also the absolute thickness of a film was measured with the touch step device. For an edge created by the evaporation of the solvent the height was 9.9 and 10.1 μm for two measurements, respectively. At an edge cut by a scalpel the height increases rapidly to 8.4 and 8.9 μm , respectively. The measurements were carried out at opposite sides of the wafer. It turned out that the thickness of the film is very homogeneous between 8.4 and 10.1 μm over a range of several centimeters.

2.4. Measuring liquids and characterization of liquids

Contact angle measurements were performed using water and glycerol, respectively. The surface tensions γ_{LV} were measured by the method of the pendant drop employing a profile analysis and found to be 64 mJ/m^2 for glycerol and 72.7 mJ/m^2 for water, respectively [7]. Water was used from a "MILLIPORE" device, whereas glycerol was used from "FLUKA Chemie AG" with a purity better than 99.5%.

3. Methods and procedures

For low rate dynamic contact angle measurements Axisymmetric Drop Shape Analysis for Profiles (ADSA-P) was applied. The experimental procedure is described in detail by Kwok in [1]. How ADSA-P works is described elsewhere [8]. The experimental set-up allows a supply of liquid to the drop from the bottom of the substrate by means of a hole. Thus, the drop can be increased very steadily and a large surface area is evaluated.

It is known that for low velocities of the three phase contact lines the contact angle is comparable to static contact angle measurements and satisfies the Young-Equation (1) /9/. In our experiments the velocity of the contact radius was in the range of 0.25 mm/min for water and 0.16 mm/min for glycerol, respectively.

Advancing contact angles at low velocity were measured starting at a drop diameter of at least 5 mm for several hundred seconds. Pictures were taken every two seconds. For each experiment a single mean and the corresponding standard deviation of the contact angle was calculated from several hundred pictures. For each copolymer, contact angles were measured on several individual substrates. Using the single means of several substrates, a general mean and the respective standard deviation for each copolymer with different side chains were calculated.

4. Results and discussion

In Table II and Table III the results are summarized. For poly(propene-*alt-N*-maleimides) the contact angle data of column 3 in Table II are given for comparison reasons and were obtained by Kwok *et al.* [15]. It can be seen that the contact angle data are nearly identical. It shows that different operators reproduce the contact angle values with very good precision. Hence, only a few measurements were performed for side chains of these lengths. For the poly(propene-*alt-N*-(*n*-dodecyl)-maleimide) with 12 carbon atoms in the side chain, nine samples were evaluated. When plotting the contact angle data versus the length of the side chain as done in Fig. 5, the trend for water and glycerol is very similar. It can be seen that the contact angle increases smoothly with increasing length of the side chain. The slope of the increase of contact angles decrease with increasing length of the side chain. When the side chain length comes to 12 carbon atoms, the slope is very flat and the contact angle reaches an upper limit. Here, the contact angle is no longer controlled by the length of the side chain, in opposite to shorter side chains. For both liquids, the maximum contact angle depends on its liquid surface tension γ_{LV} . In the graph this is made more evident by a polynomial of second order, that fits very well for both liquids. The solid surface tension γ_{SV} in Table II and Table III was calculated from the contact angle data using the "Equation of State". For the poly(propene-*alt-N*-maleimides) the solid surface tensions γ_{SV} for glycerol and water are nearly identical. This shows that the "Equation of State"-approach gives a very realistic estimation of the energetic situation of

TABLE II Summary of contact angle data and solid surface tensions γ_{SV} calculated from EQS for poly(propene-*alt-N*-maleimide) copolymers with several side chains

length of side chains	liquid	θ (degree) [15]	θ (degree)	γ_{SV} (mJ/m^2)
$m = 1$	water	69.2 ± 0.4	69.9 ± 0.8	41.7 ± 0.5
	glycerol	60.3 ± 0.4	59.5 ± 0.2	41.3 ± 0.1
$m = 3$	water	77.5 ± 0.3	78.3 ± 0.9	36.5 ± 0.5
	glycerol	70.7 ± 0.2	71.3 ± 0.1	34.6 ± 0.1
$m = 6$	water	92.3 ± 0.3	92.8 ± 0.4	27.4 ± 0.3
	glycerol	82.8 ± 0.2	81.4 ± 0.4	28.7 ± 0.2
$m = 12$	water		99.4 ± 0.7	23.4 ± 0.6
	glycerol		93.7 ± 1.9	21.8 ± 0.9

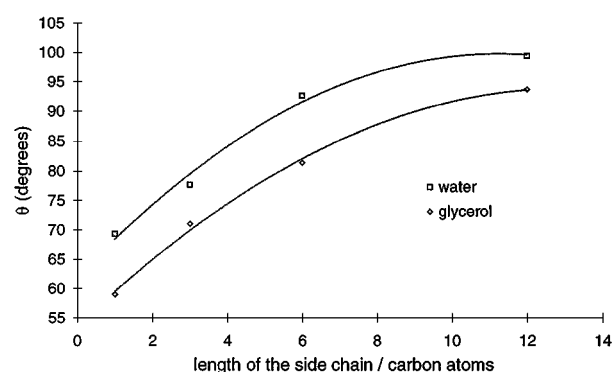


Figure 5 Contact angle data for water and glycerol on several poly(propene-*alt-N*-maleimides) versus length of the side chain.

surfaces, notwithstanding the type of liquid used. For both liquids the solid surface tensions γ_{SV} were averaged and plotted versus the length of the side chain in Fig. 6. It fits to a polynomial of second order very well. For a side chain of saturated hydrocarbon with 12 carbon atoms the solid surface tension γ_{SV} comes to 22.6 mJ/m². In the literature for a surface consisting mainly of CH₃-groups a solid surface tension γ_{SV} of 21.5 to 23 mJ/m² is reported. Zisman supposed that a surface consisting mainly of CH₃-groups has to have a critical surface tension γ_C of 21.5 mJ/m² [10]. Chen *et al.* reported a solid surface tension γ_{SV} of 23 mJ/m² for the same kind of surfaces [11]. The solid surface tension γ_{SV} of these experiments is just between. For that it is reasonable to assume that the surface is almost covered by the long saturated hydrocarbon side chains. The polar maleimide groups are shielded. To the contact angle the copolymer appears as a totally unpolar substance.

Fig. 7 shows the results of contact angle measurements versus the length of the side chain for the poly(styrene-*alt-N*-maleimide) copolymers. It is obvious that two ranges appear for the contact angle. The first range of contact angles for copolymers with no up to two carbon atoms in the side chain is about 80 degrees for water and 66 degrees for glycerol, respectively. The contact angle data was very well reproducible on several individual substrates and for different poly(styrene-*alt-N*-maleimide) copolymers as shown in Table III. The contact angle for copolymers containing different side chains shows no significant deviation. Again, for side chains consisting of four or six carbon atoms, the contact angle is constant, however, it is significantly higher. It is about 88.5 degrees for water and about 79 degrees for glycerol, respectively. This comes near to the value that is expected for polystyrene [12]. The results on individual substrates for side chains of four or six carbon atoms was very well reproducible.

For a side chain with three carbon atoms, however, the contact angle was constant on different substrates, but different contact angles were obtained for individual samples. No deviation of the surface could be realized compared to all the other copolymers investigated. Measurements were repeated by casting new films from the same copolymer solution, casting films

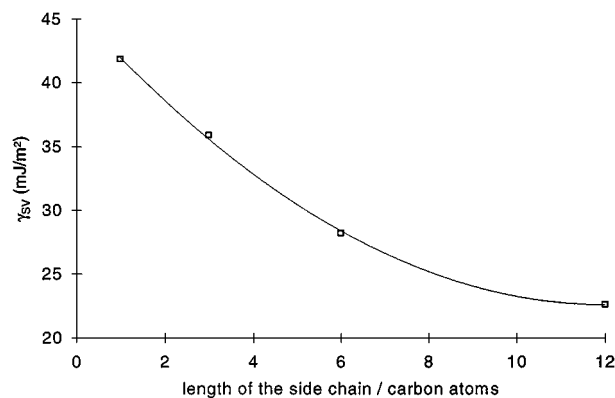


Figure 6 Solid surface tension γ_{SV} calculated using the “Equation of State” for poly(propene-*alt-N*-maleimides) versus length of the side chain.

TABLE III Contact angle data and solid-vapor surface tension γ_{SV} calculated from EQS for poly(styrene-*alt-N*-maleimide) copolymers with several side chains

length of side chains	liquid	θ (degree)	γ_{SV} (mJ/m ²)
$m = 0$	water	82.0 ± 0.5	34.2
	glycerol	65.5 ± 0.6	37.9
$m = 1$	water	79.8 ± 2.4	35.5
	glycerol	66.2 ± 1.1	37.5
$m = 2$	water	80.1 ± 0.7	35.4
	glycerol	67.9 ± 0.7	36.6
$m = 3$	water	(93.4 ± 8.1)	27.1 (?)
	glycerol	(83.8 ± 3.2)	27.4 (?)
$m = 4$	water	88.3 ± 1.2	30.2
	glycerol	80.7 ± 1.2	29.2
$m = 6$	water	88.8 ± 1.1	29.9
	glycerol	78.5 ± 0.4	30.5

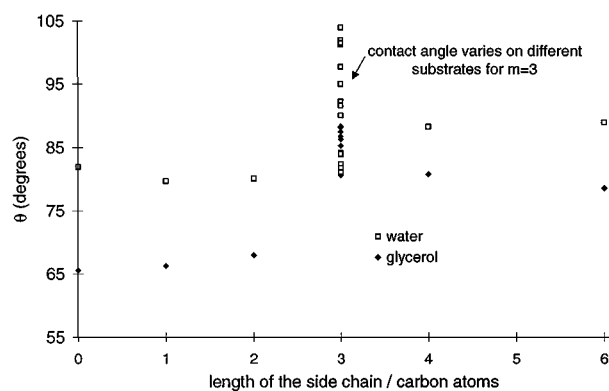
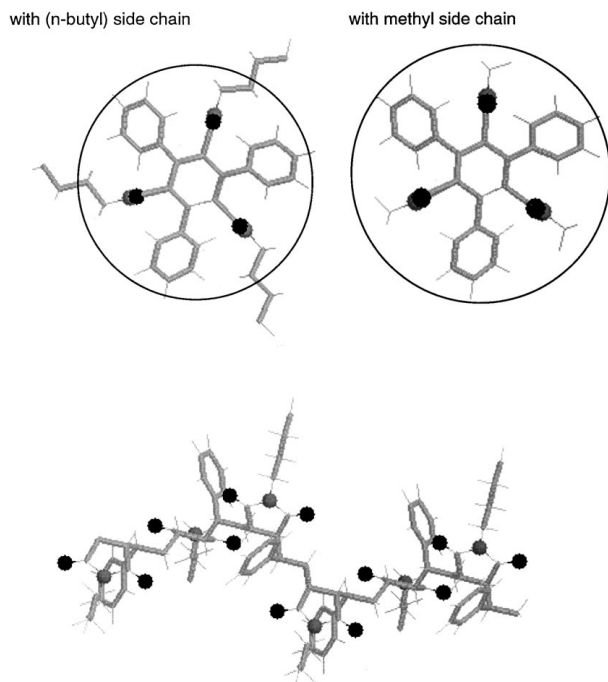


Figure 7 Plot of the contact angle data of several poly(styrene-maleimides) versus the length of the side chain.

from a new made polymer solutions as well as for a solution made of a new batch of poly(styrene-*alt-N*-(*n*-propyl)-maleimide). The contact angles on different substrates varied within 23 degrees for water and eight degrees for glycerol, respectively. That is much more than the accuracy of ADSA-P. This effect was unexpected and not consistent with the experience made for poly(propene-*alt-N*-maleimide) copolymers. It must be noticed that for a side chain length of three carbon atoms an inconsistency exists.

Another question is, why the contact angle was constant for side chains containing two, one or no carbon atoms on the one hand and for four and six carbon atoms on the other hand. One possible explanation is that the contact angle reacts very sensitively to tiny changes at the molecular level. For clarification, molecular modeling experiments were performed. It has to be mentioned that only a few macromolecules in vacuum at zero degree Kelvin were modeled. Additionally, it is not possible to take into account the energetic situation at surfaces. However, the obtained conformation of the macromolecules is very well suited as an explanation. It is displayed in Fig. 8. For better understanding the unpolar hydrogen and carbon atoms are displayed as sticks whereas the polar oxygen and nitrogen atoms are displayed as balls. It can be imagined as a two-in-one structure. The first structure is made by styrene rings, arranged in a star-like manner under an angle of 120°, around a central position. The same conformation was



key

thin bright sticks => hydrogen
 thick dark sticks => carbon
 dark balls => oxygen
 bright balls => nitrogen

Figure 8 Molecular conformation of poly(styrene-alt-*N*-maleimide) macromolecules as suggested by molecular modeling.

also suggested by Natta as energetically favorable [13]. It is obvious that this structure is favorable from an energetic point of view and necessary for steric reasons. The maleimide rings are tilted by 90 degrees relative to the styrene rings. Thus, styrene and maleimide rings do not hinder each other. Seen from the side, the structure of the macromolecule is helix-like.

The second part is built by the side chains growing from the maleimide rings in the middle between the styrene rings arranged under 120°. Longer side chains go beyond the star-like structure of the styrene rings. When drawing a circle around the styrene rings, it becomes evident that side chains up to two carbon atoms are within the radius of the star-like structure. Of course, the situation is much more complex because of energetic reasons. For example, the dominating dimension should be the van der Waals radius of this structure. Folding, tilting, orientation and interactions of the macromolecules make the situation even more complex and the exact critical radius in reality becomes unpredictable. Anyway, wherever the energetic boundary of the star-like structure will be, as long as the side chain is shorter than this critical radius, the contact angle is controlled only by the outermost, star-like styrene ring structure. Because the contact angle is a “macroscopic” property above the atomic level, it cannot realize the polar nature of the maleimide groups within the radius of the star-like structure. Therefore, changes in the length of the side chains will not influence the contact angle. However, the contact angle is greater than for comparable poly(propene-alt-*N*-maleimide) copolymers due to the hydrophobic character of the dominating styrene rings in the star-like structure. Probably, the energetic

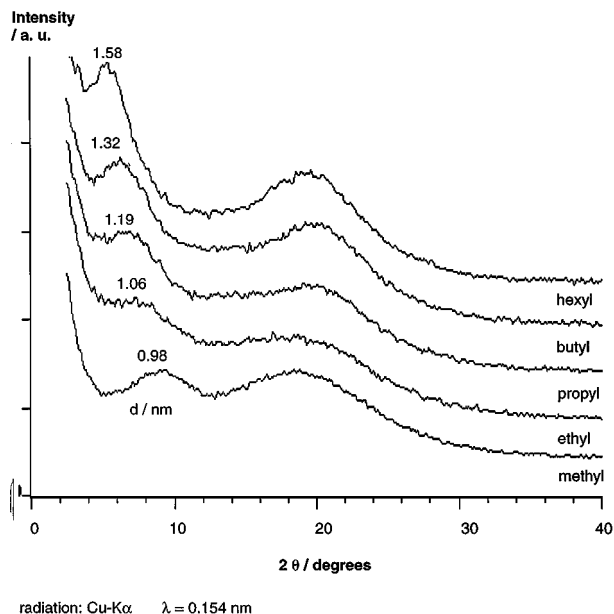


Figure 9 WAXS data plot for poly(styrene-alt-*N*-maleimides) with several side chains.

situation is very sensitively to tiny changes for a length of three carbon atoms in the side chain. Possible reasons may be the rearrangement of the side chains. So a tiny shift of the side chain length may have a huge impact on the contact angle. For side chains consisting of four or six carbon atoms, the critical radius of the star-like structure is exceeded. From now on the side chain length has an impact on the contact angle and the wetting behavior changes. However, the contact angle is not different for side chains consisting of four or six carbon atoms, because the polar maleimide groups are already shielded by styrene rings and the contact angle only detects a surface consisting of styrene rings and saturated hydrocarbon side chains.

To prove the hypothetical structure suggested by molecular modeling, WAXS experiments were performed. In Fig. 9 characteristic Bragg-peaks using arbitrary units for poly(styrene-alt-*N*-maleimides) with one to six carbon atoms in the side chains are displayed. For the experiments Cu-K α -radiation were used. For poly(styrene-alt-*N*-maleimide) without any carbon atoms in the side chain, no characteristic peak was observed. However, IR spectroscopy showed that a number of anhydride groups remained, which were not converted to maleimide groups. Anyhow, since the wetting behavior was the same like for copolymers with one and two carbon atoms in the side chain, it can be concluded that polar groups within the critical radius of the star-like styrene ring structure do not influence the wetting behavior at all. Fig. 9 shows the increase of the characteristic structure for methyl to ethyl side chains is 0.08 nm. The explanation is that the star-like styrene ring structure is stretched to give place for increasing side chains. Starting with ethyl side chains, the increase of the structure is 0.13 nm per additional carbon atom with up to six carbon atoms in the side chains. This increase corresponds exactly the space known to be required by a CH₂-group. It shows that the side chains start to extend beyond the radius of the star-like styrene ring structure anywhere between two and three carbon

atoms in the side chain and start to contribute to the wetting behavior.

5. Conclusion

It was shown that the chemical structure has a considerable impact on the contact angle values. The solid surface tension γ_{SV} decreases from 41.5 mJ/m² for poly(propene-*alt-N*-methyl-maleimide) to 22.6 mJ/m² for poly(propene-*alt-N*-(*n*-dodecyl)-maleimide). By variation of the length of the side chains, a very wide range of solid surface tension γ_{SV} is covered. Obviously the polar maleimide groups are shielded by long saturated hydrocarbon chains.

By adding a cleverly devised mixture of side chains of different length to the copolymer backbone, it should be possible to adjust any solid surface tension γ_{SV} between 22.6 and 41.5 mJ/m². The solid surface tension γ_{SV} could thus be adapted to specific applications, for example as adhesion promoters in blends or for coatings to improve the adhesion of the varnish.

On poly(propene-*alt-N*-maleimides) further investigations should be made for side chains with different polar groups at their ends. Doing this, the solid surface tension γ_{SV} is supposed to be increased above 41.5 mJ/m². However, those copolymers may become water-soluble since polar groups increase the affinity to water. If so, contact angle measurements are no longer suitable.

For poly(styrene-*alt-N*-maleimides) the wetting behavior was quite different. Not only the length of the side chains but also the chemical nature of the copolymer backbone can cause major changes in the contact angle. It was shown that the contact angle is very sensitive to tiny changes of the conformation of the polymers. Contact angle measurements can be used to detect very small changes at the macromolecular level. An explanation for the unexpected contact angle data was given using molecular modeling and was supported by WAXS-experiments. On poly(styrene-*alt-N*-maleimides) further investigations should be made employing very long side chains, for example with 12 carbon atoms. It is assumed that only small changes of the contact angle appear. Also, investigations of side chains containing polar end groups would be very interesting. Short polar side chains within the critical radius of the star-like styrene ring structure are supposed to lead to the same contact angles than those obtained for saturated hydrocarbons. Polar side chains, probably of a length of three carbon atoms, are supposed to yield considerably lower contact angles since polar groups are realized by the contact angle. For very long side chains, the contact angle is supposed to depend on the environmental situation. Storing the samples in air or vacuum, the polar groups should be buried by folding for energetic reasons as described in [14]. However, if storing the samples in a polar medium like water, the polar groups are orientated to the surface. When performing

contact angle measurements, the contact angle would decrease considerably. In this way, an additional proof for the suggested structure of the macromolecule could be given.

The roughness of the films cast from polymer solutions is less than 0.1 μm . No influence on the contact angle was detected.

Acknowledgement

The present paper reflects some findings obtained by the authors Ph.D. thesis at the "Institute of Polymer Research Dresden e. V.". The author acknowledges the support by the institute and his colleagues and would like to express his thanks for the opportunity to set up his thesis at this well-equipped research institution. Furthermore, the author wants to express his thanks to the group of Prof. A. W. Neumann, University of Toronto, for the possibility to work in the "Laboratory of Applied Thermodynamics" and learning more about dynamic contact angle measurements. The exchange to Toronto was supported by the BMBF of Germany via the GKSS Forschungszentrum GmbH, project MPT8 and the "Max-Buchner Forschungsstiftung" in Frankfurt am Main.

References

1. D. KWOK, A. LI, C. N. C. LAM, R. WU, T. GIETZELT, K. GRUNDKE, H.-J. JACOBASCH and A. W. NEUMANN, *Macromol. Chem. Phys.* **200**(5) (1999) 1121.
2. A. W. NEUMANN, R. J. GOOD, C. J. HOPE and M. SEJPAL, *J. Coll. Interf. Sci.* **49**(2) (1974) 291.
3. A. W. NEUMANN, Lecture in honor to the 60th birthday of Prof. H.-J. Jacobasch, Institute of Polymer Research, Dresden e. V., January 10, 1997.
4. H. J. BUSSCHER, A. W. J. VAN PELT, P. DE BOER, H. P. DE JONG and J. ARENDS, *Coll. & Surf.* **9** (1984) 319.
5. U. WIENHOLD, Ph.D. thesis, TU Dresden, 1994.
6. M. RÄTZSCH, S. ZSCHOCHÉ and V. STEINERT, *J. Macromol. Sci.-Chem.* **A28**(4) (1987) 949.
7. T. GIETZELT, Ph.D. thesis, TU Dresden, 1997.
8. Y. ROTENBERG, L. BORUVKA and A. W. NEUMANN, *J. Coll. Interf. Sci.* **93** (1983) 169.
9. R. V. SEDEV, C. J. BUDZIAK, J. G. PETROV and A. W. NEUMANN, *J. Coll. & Interf. Sci.* **159**(2) (1993) 392.
10. W. A. ZISMAN, *J. Am. Chem. Soc., Adv. in Chem. Series* **43** (1964) 1.
11. Y. L. CHEN, C. A. HELM and J. N. ISRAELACHVILI, *J. Phys. Chem.* **95** (1991) 10736.
12. A. AUGSBURG, K. GRUNDKE, K. PÖSCHEL, H.-J. JACOBASCH and A. W. NEUMANN, *Acta Polymerica* **49** (1998) 417.
13. G. NATTA and M. FARINA, "Struktur und Verhalten von Molekülen im Raum. Eine Einführung in die Stereochemie" (Verlag Chemie, Weinheim, Germany, 1976).
14. J. K. PIKE and T. HO, *Chem. Mater.* **8** (1996) 856.
15. D. Y. KWOK, T. GIETZELT, K. GRUNDKE, H.-J. JACOBASCH and A. W. NEUMANN, *Langmuir* **13** (1997) 2880.

Received 15 June 1999

and accepted 6 September 2000